Published in final edited form as:
J Environ Manage. 2019 March 01; 233: 489–498. doi:10.1016/j.jenvman.2018.12.060.

Health Benefit Assessment of $PM_{2.5}$ Reduction in Pearl River Delta region of China using a Model-Monitor Data Fusion Approach

Jiabin Li[1], **Yun Zhu**[1,*], **James T. Kelly**[2], **Jicheng Jang**[1], **Shuxiao Wang**[3], **Adel Hanna**[4], **Jia Xing**[3], **Che-Jen Lin**[5], **Shicheng Long**[6], **Lian Yu**[1]

[1]Guangdong Provincial Key Laboratory of Atmospheric Environment and Pollution Control, School of Environment and Energy, South China University of Technology, Guangzhou Higher Education Mega Center, Guangzhou 510006, China

[2]US EPA, Office Air Quality Planning & Standards, Research Triangle Park, NC 27711 USA

[3]State Key Joint Laboratory of Environment Simulation and Pollution Control, School of Environment, Tsinghua University, Beijing 100084, China

[4]Institute for the Environment, University of North Carolina at Chapel Hill, NC 27517 USA

[5]Department of Civil and Environmental Engineering, Lamar University, Beaumont, Texas 77710, USA

[6]Guangzhou Urban Environmental Cloud Information Technology R&D Co.ltd, Guangzhou 511400, China

Abstract

The Pearl River Delta (PRD), one of the most polluted and populous regions of China, experienced a 28% reduction in fine particulate matter ($PM_{2.5}$) concentration between 2013 (47 $\mu g/m^3$) and 2015 (34 $\mu g/m^3$) under a stringent national policy known as the Air Pollution Prevention and Control Action Plan (hereafter Action Plan). In this study, the health and economic benefits associated with $PM_{2.5}$ reductions in PRD during 2013 to 2015 were estimated using the Environmental Benefits Mapping and Analysis Program-Community Edition (BenMAP-CE) software. To create reliable gridded $PM_{2.5}$ surfaces for BenMAP-CE calculations, a data fusion tool which incorporates the accuracy of monitoring data and the spatial coverage of predictions from the Community Multiscale Air Quality (CMAQ) model has been developed. The population-weighted average $PM_{2.5}$ concentration over PRD was predicted to decline by 24%. $PM_{2.5}$-related mortality was estimated to decrease by more than 3800 due to decreases in stroke (48%), ischemic heart disease (IHD) (35%), chronic obstructive pulmonary disease (COPD) (10%), and lung cancer (LC) (7%). A 13% reduction in $PM_{2.5}$-related premature deaths from these four causes yielded a large economic benefit of about 1300 million US dollars. Our research suggests that the Action Plan played a major role in reducing emissions and additional measures should be implemented to further reduce $PM_{2.5}$ pollution and protect public health in the future.

*Correspondence to: Yun Zhu (zhuyun@scut.edu.cn).

Graphical Abstract

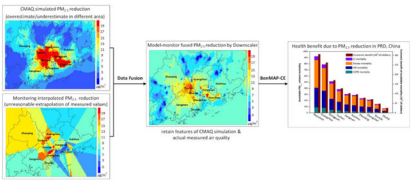

Keywords

$PM_{2.5}$-related mortality; Model-monitor data fusion; Air pollution prevention and control action plan

1. Introduction

Exposure to ambient fine particulate matter with aerodynamic diameter less than 2.5 μm ($PM_{2.5}$) has been associated with adverse human health effects including mortality (Crouse et al., 2015; Di et al., 2017a; Di et al., 2017b; Künzli et al., 2005; Pope et al., 2002) and has attracted substantial attention in China due to the extremely high $PM_{2.5}$ concentrations (Huang et al., 2014; Jung et al., 2009; Lv et al., 2017; van Donkelaar et al., 2016; Xing et al., 2017). To reduce $PM_{2.5}$ pollution, Chinese State Council has implemented air pollution control policies including Air Pollution Prevention and Control Action Plan (hereafter Action Plan; http://www.gov.cn) that aims to reduce emissions from power plants, industrial boilers, motor vehicles and fugitive dust. As reported in the Bulletin of Environmental Status, the average $PM_{2.5}$ concentration at monitors in the Pearl River Delta (PRD) region decreased from 47 $\mu g/m^3$ in 2013 to 34 $\mu g/m^3$ in 2015 (Ministry of Environmental Protection of China. http://www.mep.gov.cn). This rapid decline in $PM_{2.5}$ resulted in the PRD region achieving China's national air quality goal of 35 $\mu g/m^3$ two years ahead of the Action Plan schedule.

Policy analysts commonly rely on health benefit evaluation tools that incorporate concentration-response (C-R) functions from epidemiologic studies to assess the health benefits of air quality improvements (Maji et al., 2018; Pascal et al., 2013; U.S.EPA, 2009). In particular, the Environmental Benefits Mapping and Analysis Program-Community Edition (BenMAP-CE) developed by U.S. EPA has been widely used to estimate health benefits at the local, regional, national and global scale (Chen et al., 2017; Kheirbek et al., 2014; Sacks et al., 2018; Voorhees et al., 2014). BenMAP-CE provides three options to evaluate the cost burden of disease based on common monetary methods: willingness to pay (WTP), cost of illness (COI), and the human capital approach (HC). The WTP approach comprehensively measures the amount of money people are willing to pay for reduction in the risk of illness. The COI approach is used to measure the cost associated with health endpoints, such as medical resources used and the value of lost productivity. The HC approach measures the lost production due to illness by multiplying the period of absence by the wage rate of the absent worker (Yin et al., 2018; Yin et al., 2017). WTP is widely used for evaluating $PM_{2.5}$-related health benefits in China (Li et al., 2016; Lu et al., 2016) because it considers intangible losses, such as pain, suffering and other adverse effects due

to illness. The reliability of BenMAP-CE estimates depends on the accuracy and suitability of information used in benefit calculations such as air quality exposure fields, C-R functions, and baseline incidence rates. In previous health benefit assessments in China, the $PM_{2.5}$ exposure fields used in BenMAP-CE calculations were mostly based on chemical transport model (CTM) simulations. Predictions of CTMs, such as the Community Multiscale Air Quality (CMAQ) model, have the advantage of providing complete spatial and temporal coverage but suffer from bias compared with measured concentrations. Conversely, monitoring networks provide accurate measurements of $PM_{2.5}$ but suffer from limited coverage compared with CTM simulations. The number of $PM_{2.5}$ monitoring sites in China has recently increased from 1450 in 2013 to 1604 in 2015 (http://106.37.208.233:20035/), but the monitoring network still provides limited spatial coverage for such a large area with diverse emission sources.

Methods that combine information from $PM_{2.5}$ monitoring networks with other data sources including CTMs have recently been developed to improve exposure characterizations for health studies. For instance, Di et al. (2016) used a neural network approach to combine information from data sources including monitoring, CTMs, land use, and satellite sensors to predict daily $PM_{2.5}$ concentrations across the continental U.S. from 2000 to 2012. $PM_{2.5}$ fields for the U.S. were also developed by Beckerman et al. (2013) using a hybrid approach incorporating information from monitors, land use, traffic, and satellite retrievals in combination with CTM predictions. Zhan et al. (2017) used a spatially explicit machine learning algorithm to predict $PM_{2.5}$ concentration fields across China based on $PM_{2.5}$ monitoring, satellite, and meteorological measurements. Lv et al. (2016) developed $PM_{2.5}$ fields for North China using data from $PM_{2.5}$ monitors, satellites, and other sources (e.g., meteorological monitoring networks). These studies indicated that using hybrid models or multiple data sources could improve the accuracy of $PM_{2.5}$ prediction. Furthermore, cross-validation of $PM_{2.5}$ fields developed by multiple methods for regions in the U.S. have recently demonstrated the potential value of hybrid methods that combine information from CTMs with other data sources compared with directly using CTM output (Friberg et al., 2016; Huang et al., 2018). Both the strength of monitoring data's accuracy and CTM's spatial coverage can be integrated into prediction to reduce model biases and errors. Yet despite the advantages of combining monitor data with information from CTMs and other data sources, we are not aware of any studies that have applied air quality fields based on model-monitor fusion to estimate the benefits of air quality management in China.

In this study, we estimated the health and economic benefits associated with $PM_{2.5}$ reduction in the PRD region between 2013 and 2015 using gridded $PM_{2.5}$ fields developed by combining information from CMAQ modeling and China's monitoring network. Avoidable mortality associated with $PM_{2.5}$ reduction was estimated using BenMAP-CE with the integrated exposure-response (IER) model that provides C-R functions for the full range of ambient $PM_{2.5}$ concentrations (Apte et al., 2015; Burnett et al., 2014). To facilitate creation of the gridded $PM_{2.5}$ fields, we developed an innovative Data Fusion (DF) tool to derive spatial fields based on three algorithms commonly applied in benefit assessments: Voronoi Neighbor Averaging (VNA) (Gold et al., 1997), enhanced Voronoi Neighbor Averaging (eVNA) (Ding et al., 2016), and Downscaler (DS) (U.S.EPA, 2015, 2016). The DF tool

provides advanced capabilities for visualization and cross-validation and is available for download upon request (http://www.abacas-dss.com/abacas/Default.aspx).

2. Methodology

An overview of the analysis process for estimating health and economic benefits is provided in Figure 1. Briefly, the Weather Research and Forecasting (WRF) model was used to simulate meteorological conditions in 2013 and 2015 to drive CMAQ air quality simulations for the PRD region. Gridded $PM_{2.5}$ spatial fields for each year were then developed with the DF tool using the simulated and monitored $PM_{2.5}$. Cross-validation (CV) was done to examine the performance of the methods, and the $PM_{2.5}$ fields considered most reliable for our application were selected for input to BenMAP-CE. Finally, BenMAP-CE was applied to estimate human health and economic benefits resulting from the $PM_{2.5}$ reductions using information on population, incidence rates, and unit value for avoided deaths. Further details on the process are provided below and in the Supplementary Data.

2.1 Configuration of the WRF-CMAQ modeling system

The WRF-CMAQ modeling system used three nested modeling domains with horizontal resolutions of 27 km, 9 km and 3 km (Figure 2a). The innermost 3-km domain covers the entire PRD region for which benefits were estimated (Figure 2b). One-way nesting was used for meteorological simulations with WRF version 3.7 (http://www2.mmm.ucar.edu/wrf) and air quality simulations with CMAQ version 5.2 (http://www.epa.gov/cmaq). The initial and boundary conditions for the CMAQ simulation on the outer 27-km domain were based on default profiles in the CMAQ model. Boundary conditions for the middle 9-km and inner 3-km domains were generated from simulations on the outer and middle domains, respectively. The emission inventories for the outer and middle domains were provided by Tsinghua University, and the emission inventory for the inner 3-km domain was developed by the joint research team of Tsinghua University and South China University of Technology. Six pollutants were included in the inventories: SO_2, NO_X, CO, PM_{10}, $PM_{2.5}$ and volatile organic compounds (VOCs). Pollutant emissions decreased in the inventories between 2013 and 2015 by 57% (SO_2), 13% (NO_X) and 28% ($PM_{2.5}$). More details on emission inventories are provided in Table S1 and Table S2. $PM_{2.5}$ monitoring data over the PRD region were obtained from the Chinese Guangdong Environment Information Issuing Platform (http://www.gdep.gov.cn/). The monitoring sites are concentrated in the central urban area of PRD due to the high population, and outlying suburban areas are sparely monitored due to the low population. The implications of the monitoring network design for our study are discussed below.

The performance of the WRF model was evaluated by comparing hourly mean predicted and measured values at the Sugang and Ronggui monitoring sites. The average Pearson correlation coefficient (R) and Index of Agreement (IOA) for wind speed were about 0.5 or greater at the sites, but wind speeds were biased high (normalized mean bias, NMB: 169%) at Sugang. For relative humidity and temperature, R and IOA were greater than 0.8. For CMAQ predictions of daily mean $PM_{2.5}$, the correlation coefficient was 0.83 in 2013 and 0.86 in 2015, and predictions were slightly biased high in 2013 (NMB: 2.1%) and low in

2015 (NMB: −18.1%) (Table 1). The model performance statistics indicate that the WRF-CMAQ system had acceptable performance for our application based on consideration of statistics for CTM modeling in the U.S. (Emery et al., 2017) and our use of data fusion methods to reduce model biases and errors.

2.2 Estimating $PM_{2.5}$ with the Data Fusion tool

Annual average gridded $PM_{2.5}$ fields with 3-km horizontal resolution were developed for 2013 and 2015 over the PRD region based on algorithms of VNA, eVNA and DS using the DF tool. VNA calculates the concentration at the center of each grid cell as the inverse-distance-squared weighted average of $PM_{2.5}$ concentrations at neighboring monitors (U.S.EPA, 2017), where the neighboring monitors are identified using Delaunay triangulation. In the eVNA approach, the monitored concentrations used in VNA interpolation are multiplied by the ratio of the modeled concentration in the target grid cell to that in the monitor-containing grid cell (Ding et al., 2016). Therefore eVNA places strong weight on CMAQ gradients between the target cell and cells with nearby monitors. The DS model is a relatively complex statistical prediction model, but DS resembles a simple linear regression model with spatially varying coefficients at a high level. DS uses Markov chain Monte Carlo (MCMC) methods with Gibbs sampling to develop a relationship between observed and modeled concentrations, and then uses the relationship to predict concentrations at points in the spatial domain (Berrocal et al., 2010a, b; Rundel et al., 2015). The DS model is frequently applied in health studies (Bravo et al., 2016; Breitner et al., 2016; Warren et al., 2013). More details on the algorithms of VNA, eVNA and DS are provided in the Supplementary Data Section S2.

The annual average $PM_{2.5}$ fields were calculated as the average of fields developed for each of the four calendar quarters. The skill of the $PM_{2.5}$ prediction models was evaluated using random ten-fold CV for predictions of quarterly average concentrations. Specifically, all monitoring sites were randomly divided into groups containing 10% or 90% of the sites. Each algorithm was then applied using data from 90% of the monitoring sites to predict $PM_{2.5}$ at the remaining 10%. This process was repeated for all groups so that predictions could be evaluated against measurements at all sites. Performance was characterized using root mean square error (RMSE) and R^2 statistics as defined in Section S1. As in other recent studies (Di et al., 2016), we refer to R^2 calculated for cases including multiple samples over all sites as the total R^2.

2.3 Evaluating health and economic benefits attributable to $PM_{2.5}$ reductions

BenMAP-CE v1.3 was applied to evaluate the health and economic benefits of the $PM_{2.5}$ reductions in the PRD region between 2013 and 2015. The BenMAP-CE calculations are based on three key elements: (1) $PM_{2.5}$ fields for exposure characterization, (2) C-R functions and baseline incidence rates for health impact estimation, and (3) a unit value for willingness to pay (WTP) economic benefit estimation.

As discussed above, 3-km gridded $PM_{2.5}$ fields for 2013 and 2015 were developed using VNA, eVNA and DS methods with the DF tool. Population-weighted average $PM_{2.5}$ concentrations were calculated from these fields using population data from the 2010 China

census provided by the Data Center for Resources and Environmental Sciences, Chinese Academy of Sciences (RESDC) (http://www.resdc.cn). The 2010 census is the most recent and accurate national census and provides data at 1-km resolution that was mapped to the 3-km $PM_{2.5}$ grid for this study. Aggregated $PM_{2.5}$ concentrations referred to below are population-weighted values.

C-R functions were used to estimate $PM_{2.5}$-related health impacts in BenMAP-CE as is commonly done in human health risk assessments (Fann et al., 2013; Voorhees et al., 2011). Since previous studies have reported that mortality contributes > 90% of the health impacts of air pollution (U.S.EPA, 2011), premature mortality was selected to represent the health impacts of air pollution control in our study. The integrated exposure-response model (IER model), which provides C-R functions for the full range of ambient $PM_{2.5}$ concentrations (Burnett et al., 2014), was applied to estimate the avoidable mortality related to $PM_{2.5}$ reduction for adults (age ≥ 25) (Xujia et al., 2015). The four leading causes of death in the IER model were selected for our application: lung cancer (LC), chronic obstructive pulmonary disease (COPD), ischemic heart disease (IHD), and stroke. The C-R functions for these health endpoints are the same (Equation 1 and 2), but different parameter values are used based on the relevant studies (Table 2).

The relative risk (RR) of mortality for each health endpoint can be defined by Equation (1),

$$RR(C) = \begin{cases} 1 + \alpha\left(1 - e^{-\gamma(C - C_0)^{\delta}}\right), & if \quad C > C_0 \\ 1, & if \quad C \leq C_0 \end{cases} \tag{1}$$

where C is the average $PM_{2.5}$ concentration in 2013 or 2015; C_0 is the endpoint-specific counterfactual concentration for minimum-risk to $PM_{2.5}$; and α, γ, and δ are parameters that define the shape of the C-R curves as presented in Table 2. The premature mortality, $M_{e,g}(C_g)$, for each endpoint (e) associated with $PM_{2.5}$ in grid cell g was calculated using the RR values for 2013 and 2015 as follows:

$$M_{e,g}(C_g) = B_e \cdot P_g \cdot \frac{RR_e(C_g) - 1}{RR_e(C_g)} \tag{2}$$

where B_e represents the baseline endpoint-specific mortality incidence in the PRD region in 2013, P_g represents population in grid cell g, and $RR_e(C_g)$ is the relative risk of endpoint e for concentration C_g in grid cell g. Baseline incidence rates for the health endpoints were based on Xujia et al. (2015), which referred to governmental statistics from the Guangdong Provincial Health Statistical Yearbook (2013), and population distributions were based on the 2010 China census as described above.

The economic benefits associated with the health impact estimates were quantified using the WTP method. The unit value for avoided premature deaths was based on Xie (2011), and was adjusted by the Consumer Price Index (CPI) and exchange rate with US dollars using the 2010 currency year.

3. Results and discussion

3.1 Model validation and comparisons

$PM_{2.5}$ predictions of CMAQ were evaluated by direct comparison with measurements, and the VNA, eVNA and DS predictions were evaluated using ten-fold CV as summarized in Table 3 and Figure S1. The three DF tool algorithms had higher R^2 and lower RMSE than CMAQ in both 2013 and 2015. The high R^2 values for the DF tool algorithms were due to the high density of monitoring sites in the urban area. VNA, eVNA and DS had lower R^2 values in 2015 than 2013, whereas CMAQ predictions had higher R^2 in 2015 than 2013. Model performance differences for the years could be related to the movement of industrial point sources from the densely monitored urban area to the sparsely monitored suburban area between 2013 and 2015 (http://www.gdep.gov.cn/; Figure 3). Although the productivities of industrial sources improved during this period, the $PM_{2.5}$ filtration efficiency was relatively constant and led to increases in $PM_{2.5}$ emissions in parts of the suburban area between 2013 and 2015. The better performance for CMAQ in 2015 suggests that model performance improves with distance from the largest emission sources. The change in bias in CMAQ predictions from 2013 (NMB: 4.8%) to 2015 (NMB: −18.4%) would lead to an overestimate of the $PM_{2.5}$ change between these years. Compared with CMAQ predictions, the NMBs for the three DF tool algorithms were small and relatively constant between years.

Spatial distributions of annual $PM_{2.5}$ for the four approaches are illustrated in Figure 4. For 2013, CMAQ predicts sharp gradients between high $PM_{2.5}$ concentrations in the central urban area and relatively low concentrations in the surrounding suburban area. In contrast, CMAQ predicts relatively low $PM_{2.5}$ in the central urban area and high concentrations near point sources in the suburban area in 2015 consistent with the emission fields (Figure 3). The $PM_{2.5}$ spatial patterns for the VNA fields seem unrealistic in the suburban areas due to the extrapolation of measured values from the central monitored area to the surrounding unmonitored area. This degradation in performance away from monitors demonstrates the need to incorporate other data sources for predictions in sparsely or unmonitored areas. For the eVNA fields, relatively sharp gradients are evident compared with the other fields. These gradients are consistent with eVNA's algorithm, which applies weights based on ratios of CMAQ predictions in different spatial locations. eVNA's gradients may be beneficial in well monitored areas where emissions are well characterized but could be unreliable in unmonitored parts of the domain, and they cannot be verified in suburban areas due to the lack of monitoring. Overall, DS predictions appear to be most reliable for our application. DS performs well in CV for the central monitored area, and predictions are smooth but retain features of the CMAQ simulation in areas where monitors are not available for CV. Also, since the DS formulation does not directly involve interpolation of monitored concentrations, DS is conceptually sounder than VNA or eVNA where monitors are lacking. Therefore, DS predictions were used in our primary health benefit calculations, and CMAQ predictions were also applied to characterize the sensitivity of results to the use of data fusion.

3.2 Predicted $PM_{2.5}$ exposure level

DS predictions of changes in $PM_{2.5}$ in the PRD region between 2013 and 2015 under the Action Plan are displayed in Figure 5. Reductions in $PM_{2.5}$ ranged from −10 to 26 $\mu g/m^3$ over grid cells, and the population-weighted average $PM_{2.5}$ concentration decreased from 45 $\mu g/m^3$ to 34 $\mu g/m^3$ (a 24% reduction) (Figure 5a). The decrease in $PM_{2.5}$ predicted by DS was confirmed by the monitoring data, for which the annual mean $PM_{2.5}$ concentration decreased from 47 $\mu g/m^3$ to 34 $\mu g/m^3$ during the same period. The largest $PM_{2.5}$ reductions were observed in the most polluted regions, such as Foshan and Shenzhen. The reduction in population-weighted average $PM_{2.5}$ aggregated by city is shown in Figure 5b. During 2013 to 2015, $PM_{2.5}$ concentration decreased in all cities, with reductions greater than 10 $\mu g/m^3$ in Foshan, Shunde, Guangzhou, Shenzhen, Jiangmen and Zhongshan. Considering the $PM_{2.5}$ reductions and their spatial consistency with the change in anthropogenic emissions, the results suggest that implementation of the Action Plan played a major role in improving air quality in the PRD region.

3.3 Mortality reduction and economic benefit evaluation related to $PM_{2.5}$ concentration

We estimated health benefits for the four leading causes of $PM_{2.5}$-related premature mortality (IHD, stroke, COPD and LC). We estimated that there were about 29,600 $PM_{2.5}$-related premature adult deaths due to these four causes in the PRD region in 2013. Therefore, about 11% of the number of adult deaths in the PRD region were estimated to be associated with these $PM_{2.5}$-related health endpoints in 2013. IHD, stroke, COPD and LC contributed 45%, 44%, 7% and 4%, respectively, to the premature mortality estimate (Figure 6a). In 2013, $PM_{2.5}$-related mortality in Guangzhou, Shenzhen and Dongguan were over 4000, and the value in Guangzhou was close to 7000 (Figure 6b).

Although the number of $PM_{2.5}$-related premature adult deaths from IHD, stroke, COPD, and LC were still substantial (about 25,700) in 2015, the reduction in $PM_{2.5}$ from 2013 to 2015 led to about 3900 avoided $PM_{2.5}$-related adult deaths from these four causes. The reduction in mortality varied by endpoint consistent with the different C-R functions (Apte et al., 2015), with stroke and IHD accounting for about 48% and 35% of the avoided mortality, respectively (Figure 6c). The decrease in premature mortality from stroke and IHD was only about 14% and 10%, respectively, due to the high baseline mortality rates of stroke and IHD in 2013.

$PM_{2.5}$-related mortality reductions and economic benefits aggregated by city in 2013 and 2015 are shown in Figure 6d. Shenzhen and Guangzhou achieved mortality reductions of about 1700 with economic benefits over 570 million US dollars. The mortality reductions and economic benefits for Shenzhen, Guangzhou, Dongguan, Foshan and Jiangmen accounted for over 75% of the improvements in the PRD region. In cities with more than 5 million residents (Table 4), population-weighted $PM_{2.5}$ concentration declined by over 24% on average, which led to a mortality reduction greater than 2200 and economic benefits of about 740 million US dollars. However, in cities with relatively small population (e.g., Shunde), the avoidable $PM_{2.5}$-related mortality and economic benefits were limited (avoidable mortality < 150, economic benefit < 50 million US dollars) despite $PM_{2.5}$

reductions of 11 $\mu g/m^3$. This pattern demonstrates the strong influence of population on the health impact evaluation.

The percent reduction in $PM_{2.5}$ concentration is compared with the percent reduction in $PM_{2.5}$-related mortality in Figure 7. The relationship between percent reductions in $PM_{2.5}$ and $PM_{2.5}$-related mortality varies across cities. The highest $PM_{2.5}$ percent reduction was 29% in Foshan, where the estimated mortality reduction was 14%. Shenzhen achieved a higher percent reduction in $PM_{2.5}$-related mortality (16%) than Foshan with a smaller percent decrease in $PM_{2.5}$ concentration (28%). Apte et al. (2015) indicated that avoided mortality estimated by the IER model increases sharply with $PM_{2.5}$ at low concentrations but increases gently at higher concentrations. Therefore the marginal health benefits (i.e. mortality abatement induced by unit reduction of $PM_{2.5}$ level) increases with declines in $PM_{2.5}$ concentrations in the model.

Although Shenzhen achieved a relatively high health benefit compared to other cities due to the dense population and considerable $PM_{2.5}$ reductions, its marginal health benefits (reduction of mortality) were only 560 (per 100 thousand). Moreover, marginal health benefits for Guangzhou, Foshan and Shunde were all less than 500 (per 100 thousand), and the annual average $PM_{2.5}$ concentrations in these cities were still over than the national air quality secondary standard (35 $\mu g/m^3$) in 2015. Accordingly, the health benefits attributed to air quality improvement in the PRD region were still limited. For example, the World Health Organization (WHO) annual average $PM_{2.5}$ guideline to protect public health is 10 $\mu g/m^3$, while China's secondary standard of 35 $\mu g/m^3$ corresponds to WHO's interim target. To achieve the WHO $PM_{2.5}$ target, current policies should remain in place and additional measures should be implemented (e.g., optimization of industrial structures and the adjustment of energy structures (Dai et al., 2016; Li et al., 2017)).

To examine the influence of model-monitor fusion on health benefit estimates, we compared benefits estimated using DS fields with those estimated using CMAQ and monitor-based fields. To develop the monitor-based fields, $PM_{2.5}$ concentrations in a grid cell were assigned the concentration of the nearest monitoring site as has been considered in previous studies (Baxter et al., 2013; Hodas et al., 2013) (Table 4). In PRD, the avoided mortality using DS fields was estimated at 3886, close to the estimate of Xujia et al. (2015), which assumed that annual average $PM_{2.5}$ concentration in PRD reached the national air quality secondary standard (35 $\mu g/m^3$) in 2017 and applied the IER model to estimate the avoided deaths. The avoided mortality estimated using CMAQ fields was over than 7200, nearly two times that based on DS. The difference in avoided mortality is due to the difference in bias of CMAQ predictions for 2013 and 2015 compared with the relatively consistent and small bias for DS predictions. Specifically, CMAQ predictions were biased high in 2013 and low in 2015, and so the reduction in $PM_{2.5}$ between the years and the associated benefits would be overestimated if CMAQ output were applied directly.

The avoided mortality estimated using the nearest-site concentration assignment was about 3500 with economic benefits of about 1200 million dollars (Table 4). Therefore, in aggregate, the nearest-site approach yielded avoided mortality estimates within about 10% of the DS-based estimates. However, the spatial pattern of health benefits differed

considerably for the methods. For instance, Guangzhou achieved the highest health benefits in the nearest-site approach, but Shenzhen achieved the highest in DS. Avoided mortality estimates were 43% lower in Shenzhen for the nearest-site approach than for DS. The nearest-site approach likely underestimated concentrations in northwest Shenzhen where there are no monitors by using the relatively low concentrations measured at sites to the southeast. These limitations likely led to underestimates of avoided mortality in Shenzhen in the nearest-site approach.

Since CMAQ suffers from bias compared with measurements and the nearest-site approach provides limited spatial resolution, the model-monitor fusion approach used in this study provides a pragmatic approach to provide improved air quality surfaces for health impact assessments. More details of health benefits including VNA and eVNA are provided in Table S4.

3.4 Methodological uncertainties

There were several methodological uncertainties in our study. (1) The $PM_{2.5}$ monitoring sites are heavily concentrated in the central and southeastern parts of PRD, and the lack of monitoring in the suburban areas could limit the accuracy of predictions there. The overall benefit estimates should not be strongly influenced by these limitations though, considering that over 75% of the population was within about 10 km of a monitor and CMAQ predictions helped reduce uncertainty away from monitors. (2) The IER function was applied to estimate mortality reduction; however, the IER parameters were desired values based on 1000 simulations with 1000 sets of IER parameters from limited epidemiologic studies (Burnett et al., 2014; Xujia et al., 2015). Moreover, for stroke and IHD endpoints, the mortality reductions for adults (age ≥ 25) were estimated without age groupings, which can lead to slightly overestimated avoidable mortality (Burnett et al., 2014). (3) Baseline mortality incidence (BMI) data for 2013 was used for the entire analysis, because information on BMI variations between 2013 and 2015 is not available. (4) Population data was mapped to a 3 × 3 km grid to be consistent with the resolution of the gridded $PM_{2.5}$ fields, and population and $PM_{2.5}$ values in each grid cell were assumed to be independent and uniform. The uncertainty associated with these assumptions is believed to be small because 3-km resolution is relatively high compared with typical health impact assessments. Also, although people may have changed address between the 2010 census and the 2013–2015 study period, movement likely occurred in the core area of PRD without changing the overall population distribution. (5) Only the WTP method was used to evaluate economic benefits, and the unit value for monetization was based on studies in other regions (Xie, 2011), adjusted by CPI, due to the limited information available for the PRD region.

4. Conclusion

In this study, an innovative DF tool was developed and applied to create improved estimates of $PM_{2.5}$ distributions by combining the accuracy of monitoring data with the spatial coverage of CMAQ modeling. The model-monitor fused $PM_{2.5}$ fields were then used with BenMAP-CE to estimate the health impacts and economic benefits related to $PM_{2.5}$ reduction in the PRD region between 2013 and 2015. The study illustrates a pragmatic

approach to produce improved air quality surfaces for health benefits evaluation and is the first application of BenMAP-CE to assess the health benefits associated with $PM_{2.5}$ reduction under the implementation of Action Plan in PRD, China.

$PM_{2.5}$ concentrations in the PRD region decreased by 24% between 2013 and 2015 according to a spatial pattern consistent with emission controls implemented under the Action Plan. This behavior suggests that the Action Plan played a major role in the air quality improvement. High levels of $PM_{2.5}$ observed in the central and southeastern parts of PRD in 2013 decreased by more than 10 $\mu g/m^3$ following the emission reductions. The avoided $PM_{2.5}$-related premature mortality during 2013 to 2015 was estimated at 3886, which yielded an economic benefit of about 1300 million US dollars. However, the health benefits associated with the $PM_{2.5}$ reductions were still limited in the PRD region due to the relatively low marginal benefits under high $PM_{2.5}$ conditions. The health benefit estimates from this study strongly suggest that retain current policies and implement additional pollution control policies to further reduce $PM_{2.5}$ and protect public health.

Supplementary Material

Refer to Web version on PubMed Central for supplementary material.

Acknowledgements

This work was supported by the National Research Program for Key Issues in Air Pollution Control (No. DQGG0301), the Emissions, Air Quality, and Meteorological Modeling Support (EMAQ, EP-D-12-044), the National Key Research and Development Program of China (No. 2016YFC0207606), the Natural Science and Technology Foundation of Guangdong Province, China (No. 2016A020221001), the Outstanding Youth Fund Of National Natural Science Foundation (No. 21625701) and the Fundamental Research Funds for the Central Universities (No. D2160320&D2170150).

References

Apte JS, Marshall JD, Cohen AJ, Brauer M, 2015 Addressing Global Mortality from Ambient PM2.5. Environ. Sci. Technol 49 (13), 8057–8066. DOI: 10.1021/acs.est.5b01236. [PubMed: 26077815]

Baxter LK, Dionisio KL, Burke J, Sarnat SE, Sarnat JA, Hodas N, Rich DQ, Turpin BJ, Jones RR, Mannshardt E, Kumar N, Beevers SD, Özkaynak H, 2013 Exposure prediction approaches used in air pollution epidemiology studies: Key findings and future recommendations. J. Expos. Sci. Environ. Epidemiol 23 (6), 654–659. DOI: 10.1038/jes.2013.62.

Beckerman BS, Jerrett M, Serre M, Martin RV, Lee S-J, van Donkelaar A, Ross Z, Su J, Burnett RT, 2013 A Hybrid Approach to Estimating National Scale Spatiotemporal Variability of PM2.5 in the Contiguous United States. Environ. Sci. Technol 47 (13), 7233–7241. DOI: 10.1021/es400039u. [PubMed: 23701364]

Berrocal VJ, Gelfand AE, Holland DM, 2010a A bivariate space-time downscaler under space and time misalignment. Ann. Appl. Stat 4 (4), 1942–1975. [PubMed: 21853015]

Berrocal VJ, Gelfand AE, Holland DM, 2010b A Spatio-Temporal Downscaler for Output From Numerical Models. J. Agric. Biol. Environ. Stat 15 (2), 176–197. DOI: 10.1007/s13253-009-0004-z. [PubMed: 21113385]

Bravo MA, Anthopolos R, Bell ML, Miranda ML, 2016 Racial isolation and exposure to airborne particulate matter and ozone in understudied US populations: Environmental justice applications of downscaled numerical model output. Environ. Int 92–93, 247–255. DOI: 10.1016/j.envint.2016.04.008.

Breitner S, Schneider A, Devlin RB, Ward-Caviness CK, Diaz-Sanchez D, Neas LM, Cascio WE, Peters A, Hauser ER, Shah SH, Kraus WE, 2016 Associations among plasma metabolite levels and

short-term exposure to PM2.5 and ozone in a cardiac catheterization cohort. Environ. Int 97, 76–84. DOI: 10.1016/j.envint.2016.10.012. [PubMed: 27792908]

Burnett RT, Pope CA, Ezzati M, Olives C, Lim SS, Mehta S, Shin HH, Singh G, Hubbell B, Brauer M, Anderson HR, Smith KR, Balmes JR, Bruce NG, Kan H, Laden F, Prüss-Ustün A, Turner MC, Gapstur SM, Diver WR, Cohen A, 2014 An Integrated Risk Function for Estimating the Global Burden of Disease Attributable to Ambient Fine Particulate Matter Exposure. Environ. Health Persp 122 (4), 397–403. DOI: 10.1289/ehp.1307049.

Chen L, Shi M, Gao S, Li S, Mao J, Zhang H, Sun Y, Bai Z, Wang Z, 2017 Assessment of population exposure to PM2.5 for mortality in China and its public health benefit based on BenMAP. Environ. Pollut 221, 311–317. DOI: 10.1016/j.envpol.2016.11.080. [PubMed: 27919584]

Crouse DL, Peters PA, Hystad P, Brook JR, van Donkelaar A, Martin RV, Villeneuve PJ, Jerrett M, Goldberg MS, Pope CA, Brauer M, Brook RD, Robichaud A, Menard R, Burnett RT, 2015 Ambient PM2.5, O3, and NO2 Exposures and Associations with Mortality over 16 Years of Follow-Up in the Canadian Census Health and Environment Cohort (CanCHEC). Environ. Health Persp 123 (11), 1180–1186. DOI: 10.1289/ehp.1409276.

Dai H, Xie X, Xie Y, Liu J, Masui T, 2016 Green growth: The economic impacts of large-scale renewable energy development in China. Applied Energy 162, 435–449. DOI: 10.1016/j.apenergy.2015.10.049.

Di Q, Dai L, Wang Y, Zanobetti A, Choirat C, Schwartz JD, Dominici F, 2017a Association of short-term exposure to air pollution with mortality in older adults. JAMA 318 (24), 2446–2456. DOI: 10.1001/jama.2017.17923. [PubMed: 29279932]

Di Q, Kloog I, Koutrakis P, Lyapustin A, Wang Y, Schwartz J, 2016 Assessing PM2.5 Exposures with High Spatiotemporal Resolution across the Continental United States. Environ. Sci. Technol 50 (9), 4712–4721. DOI: 10.1021/acs.est.5b06121. [PubMed: 27023334]

Di Q, Wang Y, Zanobetti A, Wang Y, Koutrakis P, Choirat C, Dominici F, Schwartz JD, 2017b Air Pollution and Mortality in the Medicare Population. The New England journal of medicine 376 (26), 2513–2522. DOI: 10.1056/NEJMoa1702747. [PubMed: 28657878]

Ding D, Zhu Y, Jang C, Lin C-J, Wang S, Fu J, Gao J, Deng S, Xie J, Qiu X, 2016 Evaluation of health benefit using BenMAP-CE with an integrated scheme of model and monitor data during Guangzhou Asian Games. J. Environ. Sci. (China) 42, 9–18. DOI: 10.1016/j.jes.2015.06.003. [PubMed: 27090690]

Emery C, Liu Z, Russell AG, Odman MT, Yarwood G, Kumar N, 2017 Recommendations on statistics and benchmarks to assess photochemical model performance. J. Air. Waste. Manag. Assoc 67 (5), 582–598. DOI: 10.1080/10962247.2016.1265027. [PubMed: 27960634]

Fann N, Fulcher CM, Baker K, 2013 The Recent and Future Health Burden of Air Pollution Apportioned Across U.S. Sectors. Environ. Sci. Technol 47 (8), 3580–3589. DOI: 10.1021/es304831q. [PubMed: 23506413]

Friberg MD, Zhai X, Holmes HA, Chang HH, Strickland MJ, Sarnat SE, Tolbert PE, Russell AG, Mulholland JA, 2016 Method for Fusing Observational Data and Chemical Transport Model Simulations To Estimate Spatiotemporally Resolved Ambient Air Pollution. Environ. Sci. Technol 50 (7), 3695–3705. DOI: 10.1021/acs.est.5b05134. [PubMed: 26923334]

Gold CM, Remmele PR, Roos T, 1997 Voronoi methods in GIS, in: van Kreveld M, Nievergelt J, Roos T, Widmayer P (Eds.), Algorithmic Foundations of Geographic Information Systems Lecture Notes in Computer Science. Springer, Berlin, Heidelberg, pp. 21–35.

Hodas N, Turpin B, Lunden M, Baxter L, Özkaynak H, Burke J, Ohman-Strickland P, Thevenet-Morrison K, Rich DQ, 2013 Refined ambient PM(2.5) exposure surrogates and the risk of myocardial infarction. J. Expos. Sci. Environ. Epidemiol 23 (6), 573–580. DOI: 10.1038/jes.2013.24.

Huang R-J, Zhang Y, Bozzetti C, Ho K-F, Cao J-J, Han Y, Daellenbach KR, Slowik JG, Platt SM, Canonaco F, Zotter P, Wolf R, Pieber SM, Bruns EA, Crippa M, Ciarelli G, Piazzalunga A, Schwikowski M, Abbaszade G, Schnelle-Kreis J, Zimmermann R, An Z, Szidat S, Baltensperger U, Haddad IE, Prévôt ASH, 2014 High secondary aerosol contribution to particulate pollution during haze events in China. Nature 514, 218 DOI: 10.1038/nature13774. [PubMed: 25231863]

Huang R, Zhai X, Ivey CE, Friberg MD, Hu X, Liu Y, Di Q, Schwartz J, Mulholland JA, Russell AG, 2018 Air pollutant exposure field modeling using air quality model-data fusion methods and

comparison with satellite AOD-derived fields: application over North Carolina, USA. Air Quality, Atmosphere & Health 11 (1), 11–22. DOI: 10.1007/s11869-017-0511-y.

Jung J, Lee H, Kim YJ, Liu X, Zhang Y, Gu J, Fan S, 2009 Aerosol chemistry and the effect of aerosol water content on visibility impairment and radiative forcing in Guangzhou during the 2006 Pearl River Delta campaign. J. Environ. Manage 90 (11), 3231–3244. DOI: 10.1016/j.jenvman.2009.04.021. [PubMed: 19523748]

Künzli N, Jerrett M, Mack WJ, Beckerman B, LaBree L, Gilliland F, Thomas D, Peters J, Hodis HN, 2005 Ambient Air Pollution and Atherosclerosis in Los Angeles. Environ. Health Persp 113 (2), 201–206. DOI: 10.1289/ehp.7523.

Kheirbek I, Haney J, Douglas S, Ito K, Caputo S, Matte T, 2014 The Public Health Benefits of Reducing Fine Particulate Matter through Conversion to Cleaner Heating Fuels in New York City. Environ. Sci. Technol 48 (23), 13573–13582. DOI: 10.1021/es503587p. [PubMed: 25365783]

Li L, Lei Y, Pan D, Yu C, Si C, 2016 Economic evaluation of the air pollution effect on public health in China's 74 cities. SpringerPlus 5, 402 DOI: 10.1186/s40064-016-2024-9. [PubMed: 27047728]

Li Y, Chang M, Ding S, Wang S, Ni D, Hu H, 2017 Monitoring and source apportionment of trace elements in PM2.5: Implications for local air quality management. J. Environ. Manage 196, 16–25. DOI: 10.1016/j.jenvman.2017.02.059. [PubMed: 28284133]

Lu X, Yao T, Fung JCH, Lin C, 2016 Estimation of health and economic costs of air pollution over the Pearl River Delta region in China. Science of The Total Environment 566–567, 134–143. 10.1016/j.scitotenv.2016.05.060.

Lv B, Cai J, Xu B, Bai Y, 2017 Understanding the Rising Phase of the PM2.5 Concentration Evolution in Large China Cities. Sci. Rep 7, 46456 DOI: 10.1038/srep46456. [PubMed: 28440282]

Lv B, Hu Y, Chang HH, Russell AG, Bai Y, 2016 Improving the Accuracy of Daily PM2.5 Distributions Derived from the Fusion of Ground-Level Measurements with Aerosol Optical Depth Observations, a Case Study in North China. Environ. Sci. Technol 50 (9), 4752–4759. DOI: 10.1021/acs.est.5b05940. [PubMed: 27043852]

Maji KJ, Dikshit AK, Arora M, Deshpande A, 2018 Estimating premature mortality attributable to PM2.5 exposure and benefit of air pollution control policies in China for 2020. Sci. Total. Environ 612 (Supplement C), 683–693. DOI: 10.1016/j.scitotenv.2017.08.254. [PubMed: 28866396]

Pascal M, Corso M, Chanel O, Declercq C, Badaloni C, Cesaroni G, Henschel S, Meister K, Haluza D, Martin-Olmedo P, Medina S, 2013 Assessing the public health impacts of urban air pollution in 25 European cities: Results of the Aphekom project. Sci. Total. Environ 449, 390–400. DOI: 10.1016/j.scitotenv.2013.01.077. [PubMed: 23454700]

Pope CA, Burnett RT, Thun MJ, Calle EE, Krewski D, Ito K, Thurston GD, 2002 Lung Cancer, Cardiopulmonary Mortality, and Long-term Exposure to Fine Particulate Air Pollution. JAMA : the journal of the American Medical Association 287 (9), 1132–1141. DOI: 10.1001/jama.287.9.1132. [PubMed: 11879110]

Rundel CW, Schliep EM, Gelfand AE, Holland DM, 2015 A data fusion approach for spatial analysis of speciated PM2.5 across time. Environmetrics 26 (8), 515–525. DOI: 10.1002/env.2369.

Sacks JD, Lloyd JM, Zhu Y, Anderton J, Jang C, Hubbell B, Fann N, 2018 The Environmental Benefits Mapping and Analysis Program – Community Edition (BenMAP–CE): A tool to estimate the health and economic benefits of reducing air pollution. Environmental Modelling & Software 104, 118–129. DOI: 10.1016/j.envsoft.2018.02.009. [PubMed: 29962895]

U.S.EPA, 2009 Integrated Science Assessment (ISA) for Particulate Matter. U.S. Environmental Protection Agency, Washington, DC, EPA/600/R-608/139F.

U.S.EPA, 2011 The Benefits and Costs of the Clean Air Act from 1990 to 2020. U.S. EPA Office of Air and Radiation, Retrieved from: http://epa.gov/sites/production/files/2015-2007/documents/summaryreport.pdf (Accessed June 2017).

U.S.EPA, 2015 Bayesian Space-time Downscaling Fusion Model (downscaler) Derived Estimates of Air Quality for 2011. U.S. Environmental Protection Agency, Washington, DC, https://nepis.epa.gov.

U.S.EPA 2016 Technical Information about Fused Air Quality Surface Using Downscaling Tool: Metadata Description. U.S. Environmental Protection Agency, Washington, DC, https://www.epa.gov/sites/production/files/2015-2009/documents/dsmetadataair_0612_2010.pdf.

U.S.EPA, 2017 Manual and Appendices for BenMAP-CE. U.S. Environmental Protection Agency, Washington, DC, https://www.epa.gov/sites/production/files/2017-2004/documents/benmap_ce_um_appendices_april_2017.pdf

van Donkelaar A, Martin RV, Brauer M, Hsu NC, Kahn RA, Levy RC, Lyapustin A, Sayer AM, Winker DM, 2016 Global Estimates of Fine Particulate Matter using a Combined Geophysical-Statistical Method with Information from Satellites, Models, and Monitors. Environ. Sci. Technol 50 (7), 3762–3772. DOI: 10.1021/acs.est.5b05833. [PubMed: 26953851]

Voorhees AS, Fann N, Fulcher C, Dolwick P, Hubbell B, Bierwagen B, Morefield P, 2011 Climate Change-Related Temperature Impacts on Warm Season Heat Mortality: A Proof-of-Concept Methodology Using BenMAP. Environ. Sci. Technol 45 (4), 1450–1457. DOI: 10.1021/es102820y. [PubMed: 21247099]

Voorhees AS, Wang J, Wang C, Zhao B, Wang S, Kan H, 2014 Public health benefits of reducing air pollution in Shanghai: a proof-of-concept methodology with application to BenMAP. Sci. Total. Environ 485–486, 396–405. DOI: 10.1016/j.scitotenv.2014.03.113.

Warren JL, Fuentes M, Herring AH, Langlois PH, 2013 Air Pollution Metric Analysis While Determining Susceptible Periods of Pregnancy for Low Birth Weight. ISRN Obstetrics and Gynecology 2013, 9 DOI: 10.1155/2013/387452.

Xie X, 2011 Health Value: Environmental Benefit Assessment Method and Urban Air Pollution Control Strategy. Peking Univercity (PhD thesis, in Chinese).

Xing J, Wang S, Jang C, Zhu Y, Zhao B, Ding D, Wang J, Zhao L, Xie H, Hao J, 2017 ABaCAS: An Overview of the Air Pollution Control Cost–Benefit and Attainment Assessment System and Its Application in China, Environmental Managers, A&WMA.

Xujia J, Chaopeng H, Yixuan Z, Bo Z, Dabo G, Andy G, Qiang Z, Kebin H, 2015 To what extent can China's near-term air pollution control policy protect air quality and human health? A case study of the Pearl River Delta region. Environ. Res. Lett 10 (10), 104006.

Yin H, Pizzol M, Jacobsen JB, Xu L, 2018 Contingent valuation of health and mood impacts of PM2.5 in Beijing, China. Science of The Total Environment 630, 1269–1282. 10.1016/j.scitotenv.2018.02.275. [PubMed: 29554748]

Yin H, Pizzol M, Xu L, 2017 External costs of PM2.5 pollution in Beijing, China: Uncertainty analysis of multiple health impacts and costs. Environmental Pollution 226, 356–369. 10.1016/j.envpol.2017.02.029. [PubMed: 28410806]

Zhan Y, Luo Y, Deng X, Chen H, Grieneisen ML, Shen X, Zhu L, Zhang M, 2017 Spatiotemporal prediction of continuous daily PM2.5 concentrations across China using a spatially explicit machine learning algorithm. Atmos. Environ 155, 129–139. DOI: 10.1016/j.atmosenv.2017.02.023.

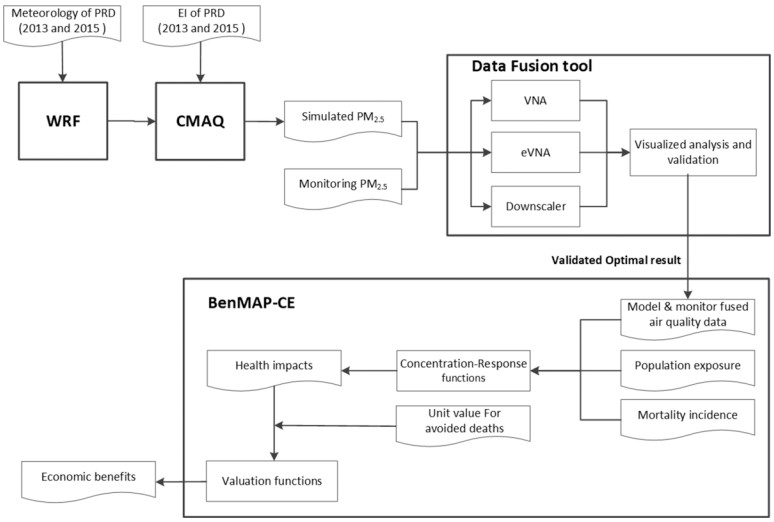

Figure 1.

Conceptual framework for model-monitor data fusion and health benefits estimate. EI: emission inventory.

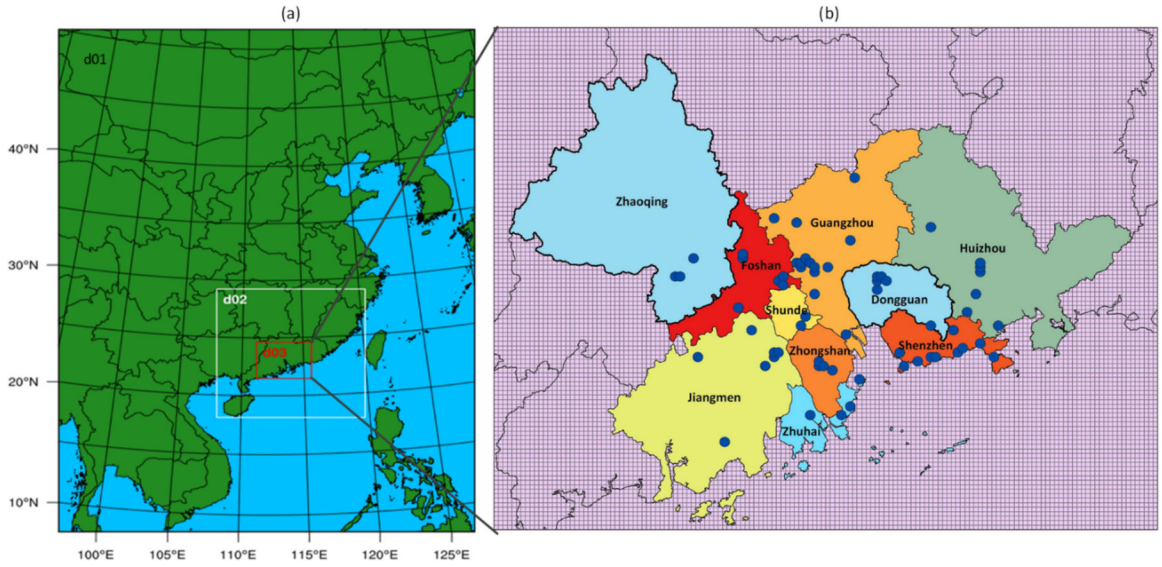

Figure 2.

(a) Nested simulation domains: 27 km (d01), 9 km (d02), and 3 km (d03); (b) Inner 3-km domain with monitor locations

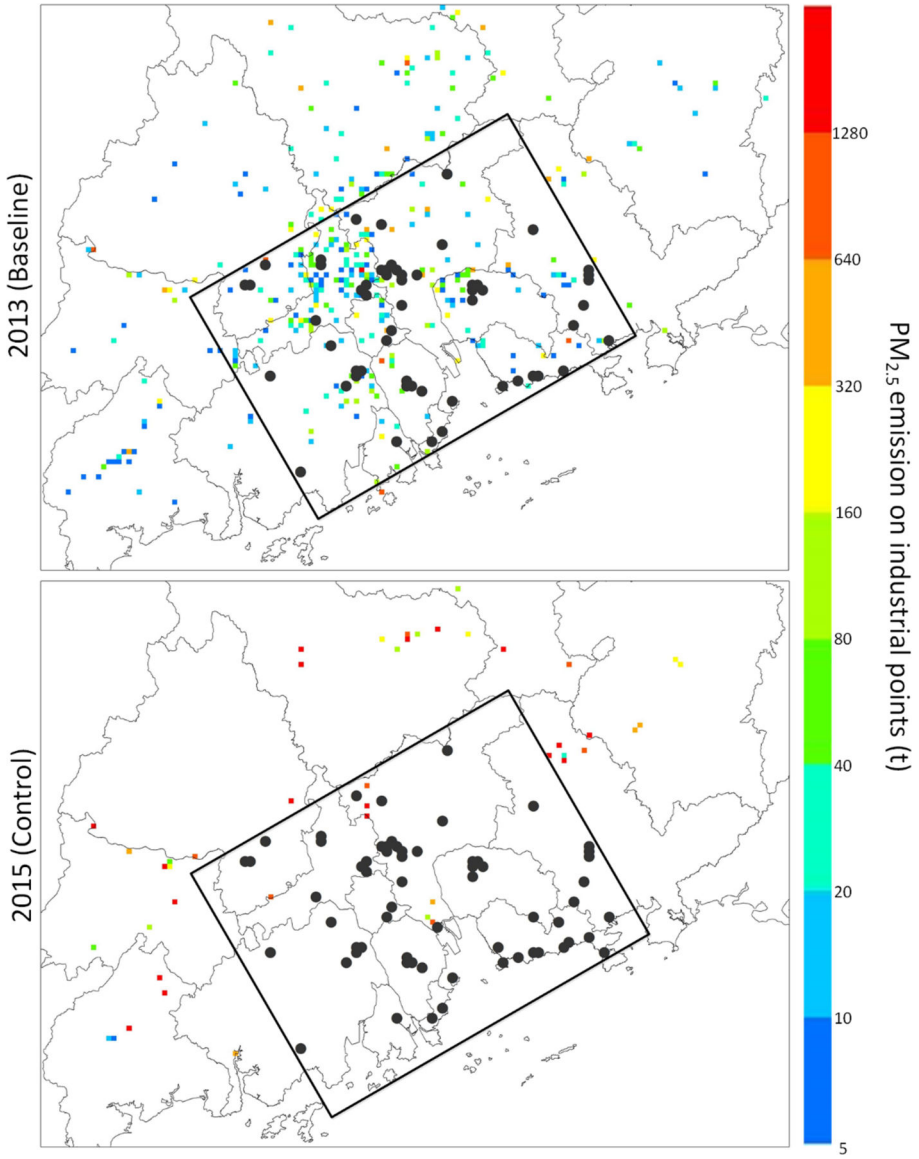

Figure 3.

$PM_{2.5}$ emissions of industrial point sources in 2013 and 2015. Note: Black circles represent the monitoring sites; Regions beyond the rectangle are unmonitored suburban parts of the PRD.

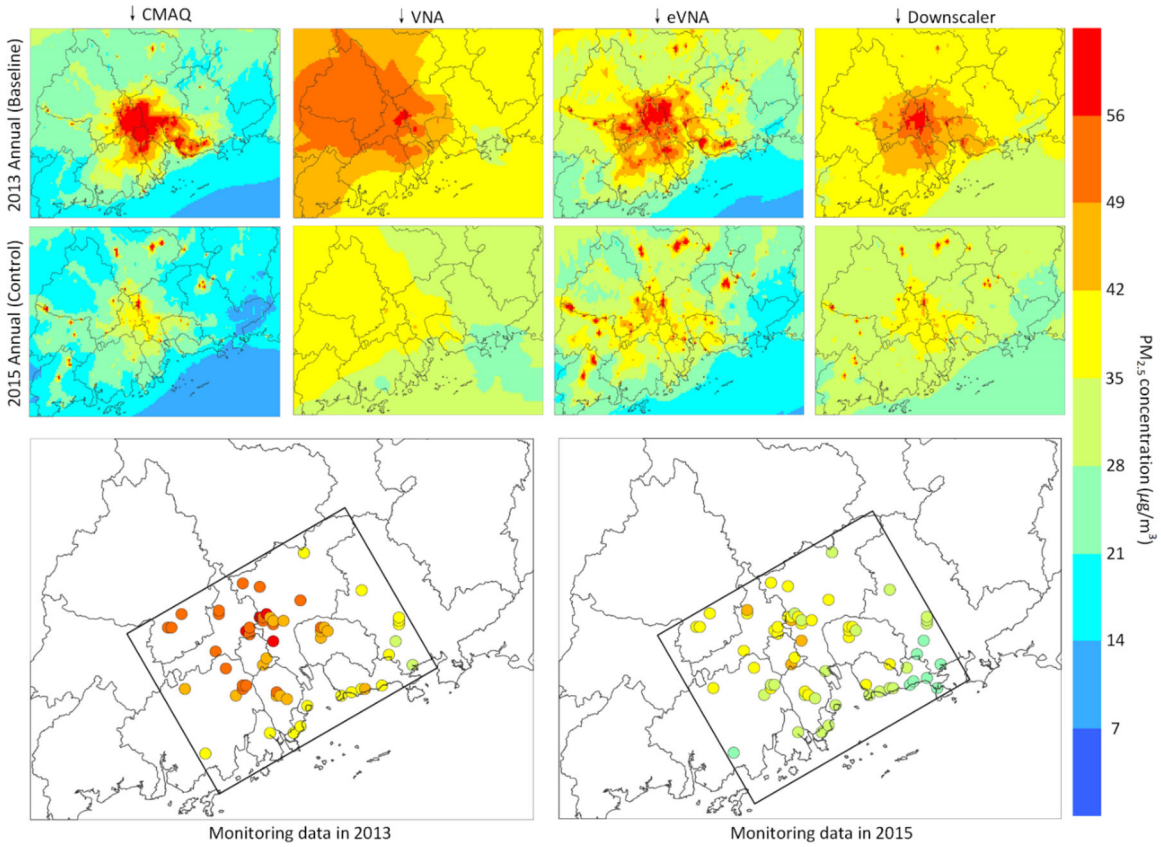

Figure 4.

Spatial distribution of CMAQ, VNA, eVNA and DS, and monitoring data. Note: Circles represent the monitoring sites; Regions beyond the rectangle are unmonitored suburban parts of the PRD.

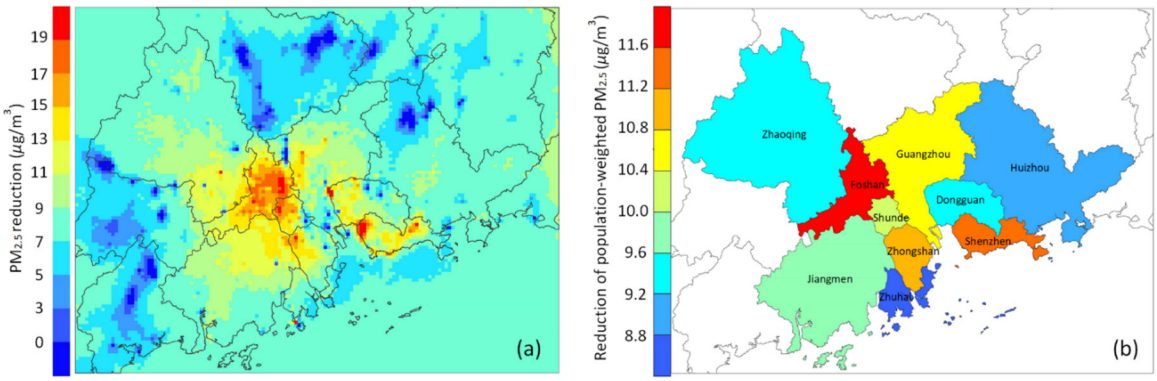

Figure 5.

(a) Spatial distribution of grid cell $PM_{2.5}$ population-weighted reduction; (b) spatial distribution of aggregated population-weighted $PM_{2.5}$ reduction.

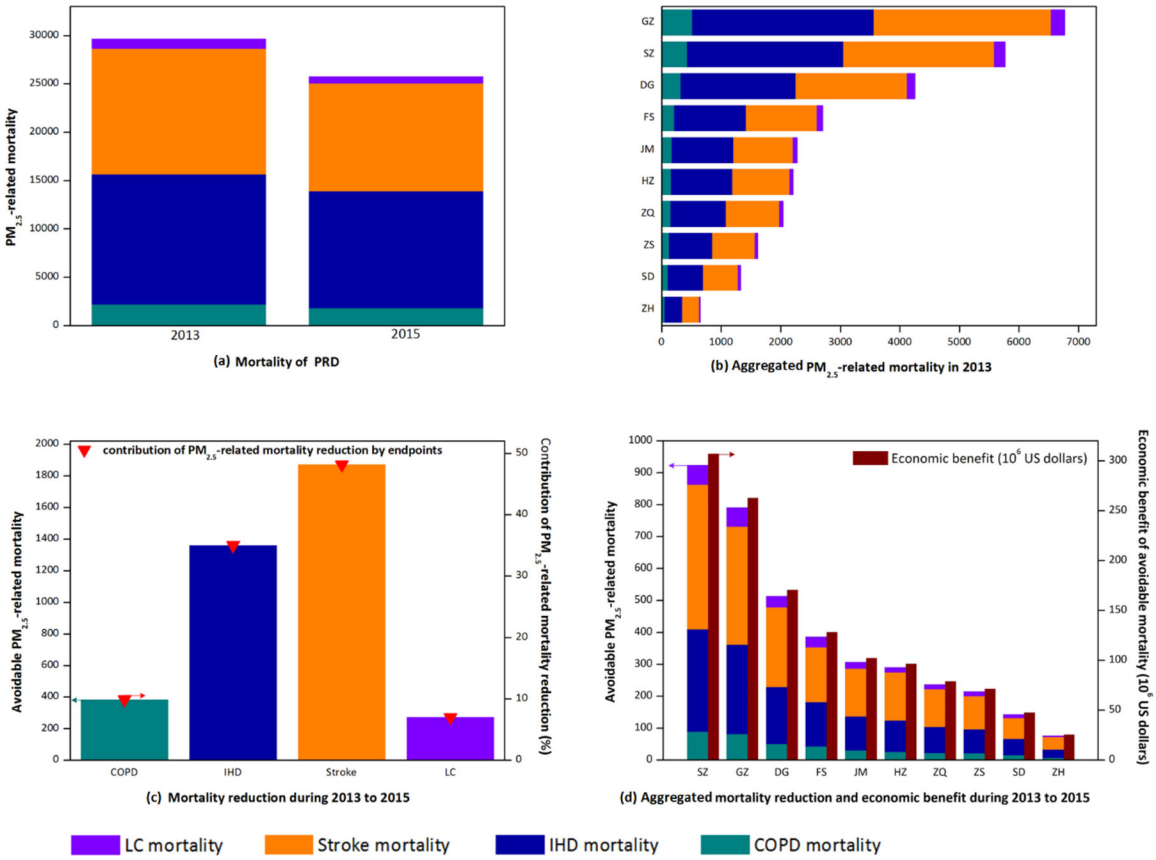

Figure 6.

(a) $PM_{2.5}$-related premature mortality of the PRD region in 2013 and 2015; (b) Aggregated $PM_{2.5}$-related premature mortality in 2013; (c) $PM_{2.5}$-related premature mortality and its contribution by endpoints during 2013–2015; (d) Aggregated avoidable premature deaths and economic benefits during 2013 to 2015

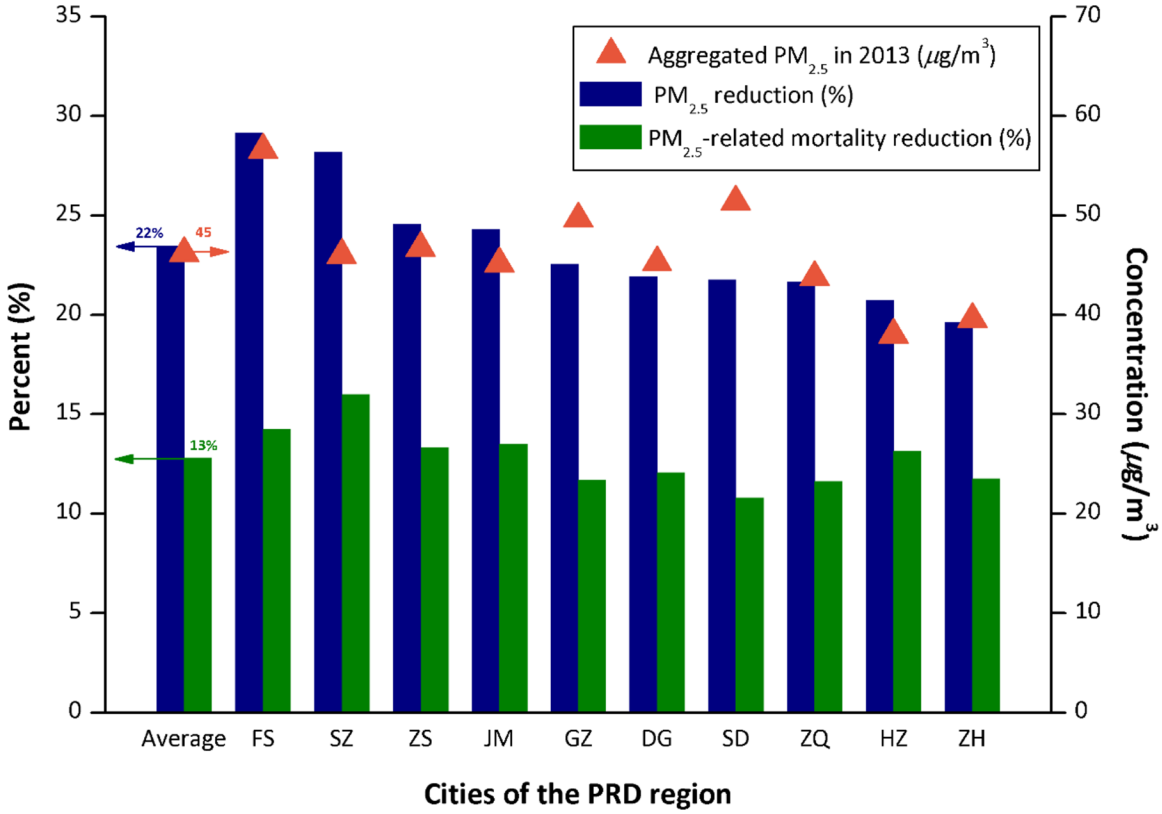

Figure 7.

Reduction of aggregated population-weighted $PM_{2.5}$ levels and reduction of $PM_{2.5}$-related mortality between 2013 and 2015. Note: (1) Blue columns and Green columns represent reductions in $PM_{2.5}$ pollution and $PM_{2.5}$-related mortality, respectively. Orange triangles is aggregated population-weighted $PM_{2.5}$ concentration in 2013. The first group of columns and triangle is the average values of all cities in the PRD region, and the other groups represent values of different cities. (2) FS - Foshan, SZ - Shenzhen, ZS - Zhongshan, JM - Jiangmen, GZ - Guangzhou, DG - Dongguan, SD - Shunde, ZQ - Zhaoqing, HZ - Huizhou, ZH - Zhuhai.

Table 1.

Comparison between monitoring data and CMAQ simulation of $PM_{2.5}$ across all monitoring sites

Year	obs_avg ($\mu g/m^3$)	model_avg ($\mu g/m^3$)	N*	Bias ($\mu g/m^3$)	NME (%)	NMB (%)	R
2013	46.7	47.7	364	1.0	22.9	2.1	0.83
2015	34.2	28.0	332	−6.2	27.8	−18.1	0.86

Note: NME and NMB is defined in Supplementary Data Section S1; obs_avg --- average observed value; model_avg --- average model value.

Table 2.

Parameters used in evaluation of health impacts and economic benefits

	Health endpoints	α	γ	δ	C_0	Baseline incidence	References
Health impacts	IHD	0.83	0.0717	0.5516	6.96	0.001212	(Burnett et al., 2014) and (Xujia et al., 2015)
	Stroke	1.01	0.0174	1.1244	8.38	0.000769	
	COPD	29.00	0.0005938	0.6786	7.17	0.0003	
	LC	33.49	0.00005013	1.0128	7.24	0.000356	

	Method	Value (thousand US dollars)	References
Economic benefits	WTP	247	(Xie, 2011)

Table 3.

Comparison of model performance statistics for CMAQ, VNA, eVNA and DS using ten-fold cross validation

Performance	2013				2015			
	CMAQ	VNA	eVNA	DS	CMAQ	VNA	eVNA	DS
total R^2	0.63	0.90	0.86	0.89	0.70	0.86	0.82	0.83
RMSE	13.1	6.0	7.4	6.3	9.8	4.2	4.9	4.7
NMB (%)	4.8	1.4	−2.1	1.4	−18.4	0.7	−0.6	0.3
slope	0.89	0.92	0.95	0.91	1.01	0.89	0.90	0.83

Table 4.

Comparison of health benefits derived from air quality change calculated by DS, CMAQ and nearest-site approach

City	Population (10^6)	Reduction of population-weighted $PM_{2.5}$ concentration ($\mu g/m^3$)			Avoidable mortality			Economic benefit (10^6 US dollars)		
		DS	CMAQ	Nearest-site	DS	CMAQ	Nearest-site	DS	CMAQ	Nearest-site
SZ	10.63	13.0	27.9	6.5	924	2149	528	307	714	175
GZ	12.93	11.2	22.5	13.4	791	1474	914	263	490	304
DG	8.32	9.9	19.0	8.8	514	1082	451	171	359	150
FS	4.80	16.5	29.0	15.2	386	610	363	128	203	121
JM	4.50	11.0	13.4	11.6	308	445	329	102	148	109
HZ	4.70	7.9	7.9	7.5	291	412	284	97	137	94
ZQ	4.02	9.5	7.6	13.8	237	253	291	79	84	97
ZS	3.17	11.5	16.5	12.7	215	344	245	72	114	82
SD	2.49	11.2	26.9	7.4	143	308	100	48	102	33
ZH	1.59	7.8	9.4	7.8	77	135	75	25	45	25
total	57.15	-	-	-	3886	7212	3580	1292	2396	1190

Note: SZ - Shenzhen, GZ - Guangzhou, DG - Dongguan, FS - Foshan, JM - Jiangmen, HZ - Huizhou, ZQ - Zhaoqing, ZS -Zhongshan, SD - Shunde, ZH - Zhuhai